Journal of Solid State Chemistry **146,** 277–286 (1999)
Article ID jssc.1999.8375, available online at http://www.idealibrary.com on IDEAL®

Synthesis, Crystal Structure, Electrical, and Magnetic Properties of the New Layered Cobalt Oxides $(Sr, Ca, Ln)_3Co_2O_{6\pm\delta}$ (Ln = Sm, Eu, Gd, Tb, Dy, Ho, and Y)

K. Yamaura,*,[1] Q. Huang,†,‡ and R. J. Cava*

*Department of Chemistry and Princeton Materials Institute, Princeton University, Princeton, New Jersey 08540; †NIST Center for Neutron Research, National Institute of Standards and Technology, Gaithersburg, Maryland 20899; and ‡Department of Materials and Nuclear Engineering, University of Maryland, College Park, Maryland 20742

Received January 28, 1999; in revised form April 12, 1999; accepted May 10, 1999

New layered Co oxides of nominal formula $Sr_2(Ln_{0.8}Ca_{0.2})Co_2O_6$ (Ln = Sm, Eu, Gd, Tb, Dy, Ho, and Y) are reported. Single-phase polycrystalline samples were obtained at compositions $Sr_2Y_{1-x}Ca_xCo_2^{2.5+}O_{6-\delta}$ ($0.2 \le x \le 0.5$; $0 \le \delta \le 0.24$), $Sr_2Y_{1-x}Ca_xCo_2^{3.4+}O_{6+\delta'}$ ($0.2 \le x \le 0.5$; $0.62 \le \delta' \le 0.79$), and $Sr_2Dy_{0.8}Ca_{0.2}Co_2O_{6.09}$. Powder X-ray and neutron diffraction, thermogravimetric analysis, magnetic susceptibility, and ac resistivity measurements were used to characterize the samples. The tetragonal unit cell for $Sr_2Y_{0.8}Ca_{0.2}Co_2O_{6.00}$ ($I4/mmm$; a = 3.82765(6) Å, and c = 19.5795(3) Å) is comparable to that of the double layer superconducting copper oxide $La_{2-x}Sr_xCaCu_2O_6$. A long-range antiferromagnetic (AF) ordered state below about 300 K is found for $Sr_2Y_{1-x}Ca_xCo_2^{2.5+}O_{6-\delta}$, and a magnetically glassy state below about 40 K for the oxidized AF phases. All materials are electrically insulating. © 1999 Academic Press

Key Words: **$Sr_2(Ln, Ca)Co_2O_6$; $La_{2-x}Sr_xCaCu_2O_6$; layered structure; spin glass; Kohlrausch law.**

INTRODUCTION

Since high-T_c superconductivity was discovered in two dimensional (2D) strongly correlated electronic materials, such materials have been of great interest. The superconductivity is believed to be distinctly related to the 2D nature. In order to shed insight into the behavior of 2D electronic solids, and find new phenomena derived from their 2D nature, tremendous efforts have been made to discover new lower dimensional strongly correlated electronic materials. Almost all 2D superconducting materials found thus far are based on layered copper oxides consisting of CuO_2 sheets and spacer and charge reservoir layers. A variety of structurally 2D superconductors, e.g., $NbSe_2$ (1), Sr_2RuO_4 (2), and LnT_2B_2C (Ln, rare earth element; T = Ni, Pd, and Pt) (3–5) are known. The superconducting transition temperatures are, however, quite low when compared with those of the cuprates. Moreover, the superconducting properties are quite different (6, 7), e.g., odd parity superconductivity has been suggested for Sr_2RuO_4 (6), and 3D superconducting properties were found in LnT_2B_2C (7). A new family of structurally 2D copper-free superconductors with structures related to the cuprates would be of great interest in helping to elucidate the microscopic mechanism for cuprate superconductivity.

Here we report new CoO_2-layered tetragonal Co oxides of nominal formula $Sr_2Ln_{0.8}Ca_{0.2}Co_2O_6$ (Ln = Sm, Eu, Gd, Tb, Dy, Ho, and Y). Single-phase polycrystalline samples $Sr_2Y_{1-x}Ca_xCo_2O_{6-\delta}$ ($0.2 \le x \le 0.5$; $0 \le \delta \le 0.24$) and $Sr_2Dy_{0.8}Ca_{0.2}Co_2O_{6.09}$ were obtained. These phases are isostructural with the double layer superconducting copper oxide $La_{2-x}Sr_xCaCu_2O_6$ (T_c = 60 K) (8). The powder neutron diffraction (ND) pattern at room temperature of $Sr_2Y_{0.8}Ca_{0.2}Co_2O_{6.00}$ has been refined to good agreement (R_p = 4.07%, R_{wp} = 4.71%), by means of the Rietveld technique, with a structural model based on $La_{2-x}Sr_xCaCu_2O_6$. The tetragonal unit cell ($I4/mmm$, a = 3.82765(6) Å, and c = 19.5795(3) Å) of $Sr_2Y_{0.8}Ca_{0.2}Co_2O_{6.00}$ is comparable with that of the analogous copper oxide ($I4/mmm$, a = 3.821 Å, and c = 19.60 Å) (8). The CoO_2 layers have Co ions in pyramidal coordination, as is also found in the copper oxide.

$Sr_2Y_{1-x}Ca_xCo_2^{2.5+}O_{6-\delta}$ ($0.2 \le x \le 0.5$; $0 \le \delta \le 0.24$) was found to be antiferromagnetic. Increasing the formal Co valence from +2.5 to +3.4 by increasing the oxygen content switches the magnetic state from a long range ordered AF state to a magnetically glassy state. No traces of superconductivity were found down to 5 K for any of the samples. The synthesis, crystal structure, electrical, and magnetic properties of the new phases are introduced in this article.

[1]To whom correspondence should be addressed. Email: yama@princeton.edu

0022-4596/99 $30.00

EXPERIMENTAL

Polycrystalline samples were synthesized and characterized as follows. Mixtures (2 grams each) of $SrCO_3$ (99.99%), Y_2O_3 (99.999%), $CaCO_3$ (99.95%), and Co_3O_4 (99.9985%) with ratios $Sr:Y:Ca:Co = 2:1-x:x:2$ ($x = 0$ to 1 with a 0.1 step) were heated at 800°C for 24 hours in nitrogen. After grinding, the preheated mixtures were heated again at 1000°C for 24 hours in nitrogen. After another grinding, heating was repeated at 1100°C. The samples were then ground, pressed into pellets, and heated at 1200°C in nitrogen for 24 hours. The final step, grinding, presssing, and heating at 1200°C, was repeated. Alumina crucibles were employed. Mixtures with each of the following rare earth oxides, at $x = 0.2$, were also prepared and treated with the above synthesis conditions: Nd_2O_3 (99.9%), Sm_2O_3 (99.9%), Eu_2O_3 (99.9%), Gd_2O_3 (99.999%), Tb_4O_7 (99.9%), Dy_2O_3 (99.99%), Ho_2O_3 (99.9%), and Er_2O_3 (99.99%). A large quantity of sample (12 grams in the starting mixture) was made for the powder ND study; for the composition $Sr_2Y_{0.8}Ca_{0.2}Co_2O_z$, was also made as described above. Two of the single-phase samples, $Sr_2Y_{0.8}Ca_{0.2}Co_2O_{5.92}$ and $Sr_2Y_{0.5}Ca_{0.5}Co_2O_{5.76}$, were annealed at 430°C in oxygen at 31.4 MPa for 48 hours to test for the effect of excess oxygen accommodation.

Powder X-ray diffraction (XRD), with Cu$K\alpha$ radiation at room temperature, and thermogravimetric analyses (TGA) were employed to characterize the samples. A small amount of fine nickel powder was mixed with each ground sample as an internal standard in the XRD study. The oxygen content of selected samples was determined by reduction to alkaline earth monoxides, rare earth oxide, and Co metal in the TGA by heating in 10% hydrogen/90% nitrogen at a heating rate of 5 K per minute to 800°C and holding for 8 hours. A SQUID magnetometer (Quantum Design MPMS5) was employed to study the magnetic properties of selected samples between 5 and 400 K. The highest applied magnetic field was 55 kOe. The electrical resistivity was measured between 77 and 400 K by a conventional four-probe ac technique with a gauge current of 10 μA at 132 Hz.

The powder ND study for the representative polycrystalline single-phase sample, $Sr_2Y_{0.8}Ca_{0.2}Co_2O_{6.00}$, was performed at National Institute of Standards and Technology Center for Neutron Research. The BT-1 high-resolution diffractometer was employed. The intensity of diffracted monochromatic neutrons of wavelength of 1.5402(1) Å was measured at diffraction angles between 3 and 168 degrees with a 0.05-degree step size. Collimators with horizontal divergences of 15′, 20′, and 7′ of arc were used before and after the Cu (3 1 1) monochromater and after the sample, respectively. The data were collected at 295 K. Structural refinement calculation by means of the Rietveld technique was carried out with the program GSAS (9). The neutron scattering amplitudes used in the refinements were 0.702, 0.775, 0.490, 0.353, and 0.581 ($\times 10^{-12}$ cm) for Sr, Y, Ca, Co, and O, respectively (9).

STOICHIOMETRY AND STRUCTURE

The powder XRD patterns of the samples as made are presented in Figs. 1 and 2. Figure 1 shows the XRD patterns for samples with the nominal formula $Sr_2Y_{1-x}Ca_xCo_2O_6$ ($0 \le x \le 1$ with a 0.1 step). The figure shows that single-phase samples were obtained for x values between 0.2 and 0.5. The $x = 0.2$ composition was selected to test for the existence of the phase for different lanthanides. The results are summarized in Fig. 2 for the lanthanides Nd–Er. The phase is seen to be present as the major phase for the lanthanides Sm through Ho, with single-phase material obtained for Dy, and nearly for Ho, which have ionic radii approximately equal to that of Y. Figure 2 also shows that the phase does not form for Nd and Et, and, for other lanthanides, the phase was not observed at all.

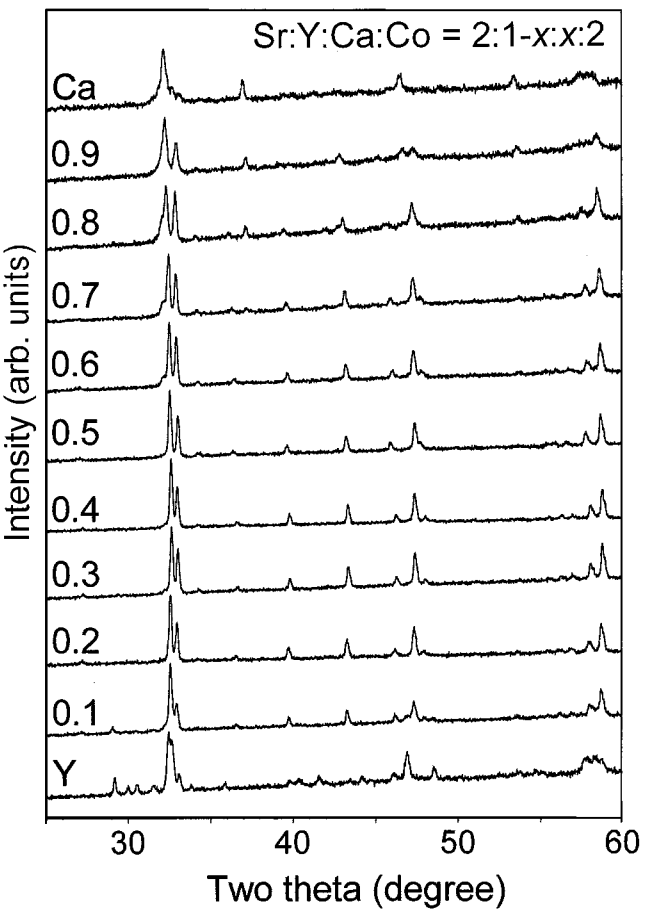

FIG. 1. The powder XRD patterns at room temperature of samples as made in nitrogen with nominal formula $Sr_2Y_{1-x}Ca_xCo_2O_6$ ($0 \le x \le 1$). Numbers beside left vertical axis, above each pattern, represent the value of x. The solid solution is found to be single phase for $0.2 \le x \le 0.5$.

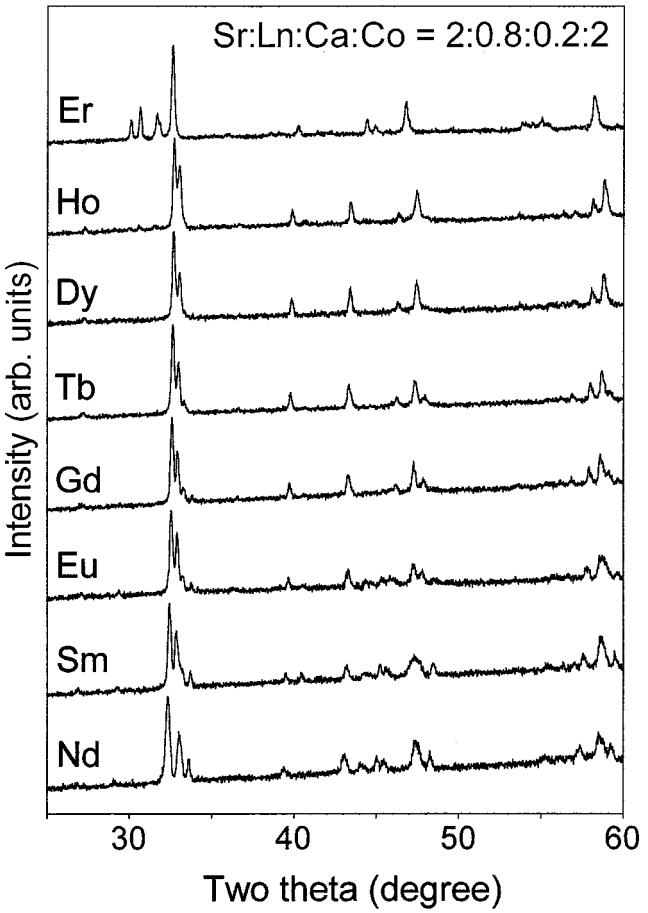

FIG. 2. The powder XRD patterns at room temperature of samples as made in nitrogen with nominal formula $Sr_2Ln_{0.8}Ca_{0.2}Co_2O_6$ (Ln = Nd, Sm, Eu, Gd, Tb, Dy, Ho, and Er). Stoichiometric single-phase polycrystalline samples are obtained for Dy and nearly for Ho.

All peaks in each XRD pattern of the single-phase samples can be indexed by a tetragonal unit cell. For example, all observed peaks for $Sr_2Y_{0.8}Ca_{0.2}Co_2O_6$, listed in Table 1, are indexed by the body centered tetragonal unit cell with lattice constants $a = 3.828(1)$ Å and $c = 19.61(1)$ Å. Many peaks in the XRD patterns of the multiple-phase samples can be indexed by analogy. Lattice constants determined by least squares fitting of the peak positions, and volumes of the tetragonal unit cell derived from those lattice constants, are plotted in Figs. 3 and 4 for $Sr_2Y_{1-x}Ca_xCo_2O_6$ and $Sr_2Ln_{0.8}Ca_{0.2}Co_2O_6$, respectively.

Even though the materials at many of the compositions are multiple phase, systematic behavior is observed over the tested composition range, especially seen in the rare earth series, in which the cell size clearly increases with lanthanide radius (r_{Ln}). Thus the new phase forms for an intermediate range of lanthanide radii (1.004 Å $< r_{Ln} <$ 1.109 Å (10)), but is only single phase or nearly single phase at the compostition $Sr_2Ln_{0.8}Ca_{0.2}Co_2O_6$ for the narrow range of radii between Y and Ho (1.015 Å $< r_{Ln} <$ 1.040 Å (10)). For the non-single-phase compositions, there may be a different type of nonstoichiometry present than what was explored here. The possibility of substitution for Co by the other element(s) is negligible due to a large difference in ionic radius (10). We speculate that the nonstoichiometry may involve the presence of Ca on the Sr site, in a formula of the type $(Sr_{2-x}Ca_x)(Ln_{1-y}Ca_y)Co_2O_6$. We have not studied that type of nonstoichiometry here, but believe it might be of interest in the future.

For the single-phase Y sample at $x = 0.2$, a total oxygen content of 5.92 per formula unit (f.u.), i.e., $Sr_2Y_{0.8}Ca_{0.2}Co_2O_{5.92}$, was found by the TGA analysis, although 6.00 per f.u. is expected for the ideal structure, in analogy to $La_{2-x}Sr_xCaCu_2O_6$ (8). For one of the other single-phase Y samples, at $x = 0.5$, a total of 5.76 oxygens per f.u, i.e., $Sr_2Y_{0.5}Ca_{0.5}Co_2O_{5.76}$, were found in the TGA analysis, indicating that about 4% of the oxygen are missing from the ideal stoichiometric composition. The formal valence of Co calculated from the formulae $Sr_2Y_{0.8}Ca_{0.2}Co_2O_{5.92}$ and $Sr_2Y_{0.5}Ca_{0.5}Co_2O_{5.76}$ are +2.51 and +2.52, respectively, suggesting that the Co valence of 2.5 + is strongly favored for this system under the synthetic conditions employed.

TABLE 1
Observed XRD Peaks of $Sr_2Y_{0.8}Ca_{0.2}Co_2O_{5.92}$ at Room Temperature

h	k	l	d_{obs} (Å)	d_{cal} (Å)	I/I_{105} (%)
1	0	1	3.756	3.757	6
1	0	3	3.302	3.304	1
0	0	6	3.270	3.269	4
1	0	5	2.739	2.740	100
1	1	0	2.706	2.707	49
1	1	2	2.612	2.609	4
0	0	8	2.450	2.452	6
1	1	4	2.371	2.370	1
1	0	7	2.261	2.261	13
1	1	6	2.086	2.085	24
0	0	10	1.962	1.961	9
2	0	0	1.915	1.914	35
1	0	9	1.893	1.894	3
2	0	2	1.876	1.879	1
1	1	8	1.816	1.817	1
2	0	4	1.782	1.783	2
2	1	1	1.705	1.706	3
2	1	3	1.655	1.656	2
2	0	6	1.652	1.652	3
0	0	12	1.635	1.635	4
1	0	11	1.616	1.616	5
1	1	10	1.588	1.588	12
2	1	5	1.570	1.569	32
2	0	8	1.509	1.509	2

Note. All peaks can be indexed by a tetragonal unit cell with lattice constants $a = 3.828(1)$ Å, and $c = 19.61(1)$ Å. Indices (h, k, and l), observed interplanar spacing (d_{obs}), calculated interplanar spacing (d_{cal}), and normalized observed internsity (I/I_{105}) are given.

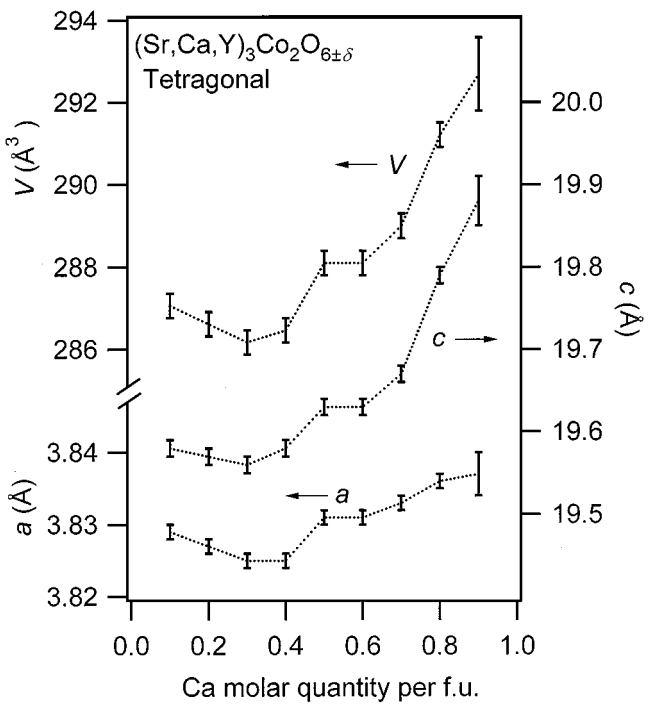

FIG. 3. Lattice constants (a and c) and unit cell volume (V) of the tetragonal phase (Sr, Ca, Y)$_3$Co$_2$O$_{6\pm\delta}$. The nominal formula is $Sr_2Y_{1-x}Ca_xCo_2O_6$ ($0 \le x \le 1$).

Although single-phase samples were made at $0.2 \le x \le 0.5$, the most oxygen-stoichiometric materials were obtained at $x = 0.2$. The nonlinear relation between the lattice constants and the Ca content (Fig. 3) is likely to be related to the variation in oxygen stoichiometry with Ca content. The TGA analysis for the Dy sample revealed a superstoichiometric oxygen content of 6.09 per f.u, i.e., $Sr_2Dy_{0.8}Ca_{0.2}Co_2O_{6.09}$. Thus the total oxygen content may be either slightly less or slightly more than 6 per f.u. and is dependent on the radii of the component large ions, as is observed in the related copper phases $La_{2-x}Sr_xCaCu_2O_{6\pm\delta}$ and $La_{2-x}Sr_{1+x}Cu_2O_{6\pm\delta}$ (11). The exact value is also sensitive to the details of the synthetic condition, including the overall size of the sample.

To determine the structure of the tetragonal phase, one of the single-phase samples, $Sr_2Y_{0.8}Ca_{0.2}Co_2O_{6.00}$, was studied by powder ND. In Fig. 5, the observed powder ND pattern obtained at 295 K is presented with the pattern calculated for the final structural model. The refined structural parameters are presented in Table 2. All observed peak positions, indicated by small vertical bars below the patterns, are clearly reproduced by the calculation, indicating the quality of the sample. A body centered tetragonal unit cell ($I4/mmm$, $a = 3.82765(6)$ Å, and $c = 19.5795(3)$ Å) was found. The agreement factors, 4–5% (Table 2) indicate the high quality of the refinements. Several structural refinements were employed to test the possible nonstoichiometry of the phase. The partial substitution for Sr by the other element(s), and excess oxygens at the interstitial $2a(0,0,0)$ site, which is in Y/Ca layer, were investigated; however, the refinements indicated that those did not occur. The occupancy factor of the oxygens in the normally occupied sites at $4i(0,0,z)$ and $8g(0,1/2,z)$ refined to within one standard deviation of 1.00, and the sites are therefore taken to be fully occupied. The composition of the tetragonal phase studied in the ND experiment was therefore stoichiometric $Sr_2Y_{0.8}Ca_{0.2}Co_2O_{6.00}$ in agreement with the nominal concentration. Because the oxygen content of the ND sample is somewhat different from that of the sample tested in the TGA, 5.92 per f.u., a study of the oxygen stoichiometry as a function of synthetic conditions may be of further interest. A structural view of the tetragonal phase is drawn in Fig. 6, based on the result of the powder ND study. Selected interatomic distances and bond angles calculated from the structural parameters are listed in Table 3. The CoO_5 pyramid has slightly longer in-plane distances, 1.96 Å, than to the apical oxygen, 1.93 Å. The CoO_2 layer is not flat (Fig. 7). The O(2)–Co–O(2) angle is 154 degrees, far from the ideal 180 degrees. There is no rotation of the pyramids around their shared corners.

The formal valence of Co of +2.51 for $Sr_2Y_{0.8}Ca_{0.2}Co_2O_{5.92}$ and +2.52 for $Sr_2Y_{0.5}Ca_{0.5}Co_2O_{5.76}$ increased to +3.39, i.e., $Sr_2Y_{0.8}Ca_{0.2}Co_2O_{6.79}$, and +3.37, i.e., $Sr_2Y_{0.5}Ca_{0.5}Co_2O_{6.62}$, respectively, after the post annealing

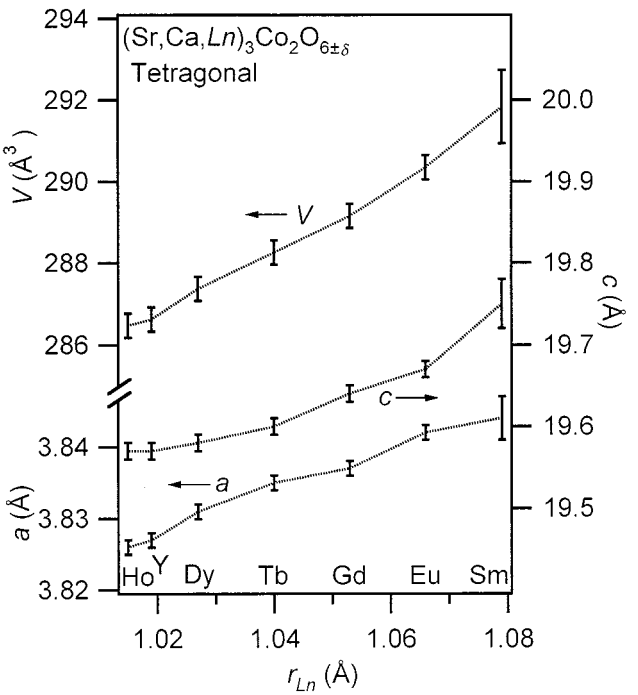

FIG. 4. Lattice constants (a and c) and unit cell volume (V) of the tetragonal phase (Sr, Ca, Ln)$_3$Co$_2$O$_{6\pm\delta}$ (Ln rare earth element). The nominal formula is $Sr_2Ln_{0.8}Ca_{0.2}Co_2O_6$. The horizontal axis represents the effective ionic radius of the rare earth elements (r_{Ln}) (10).

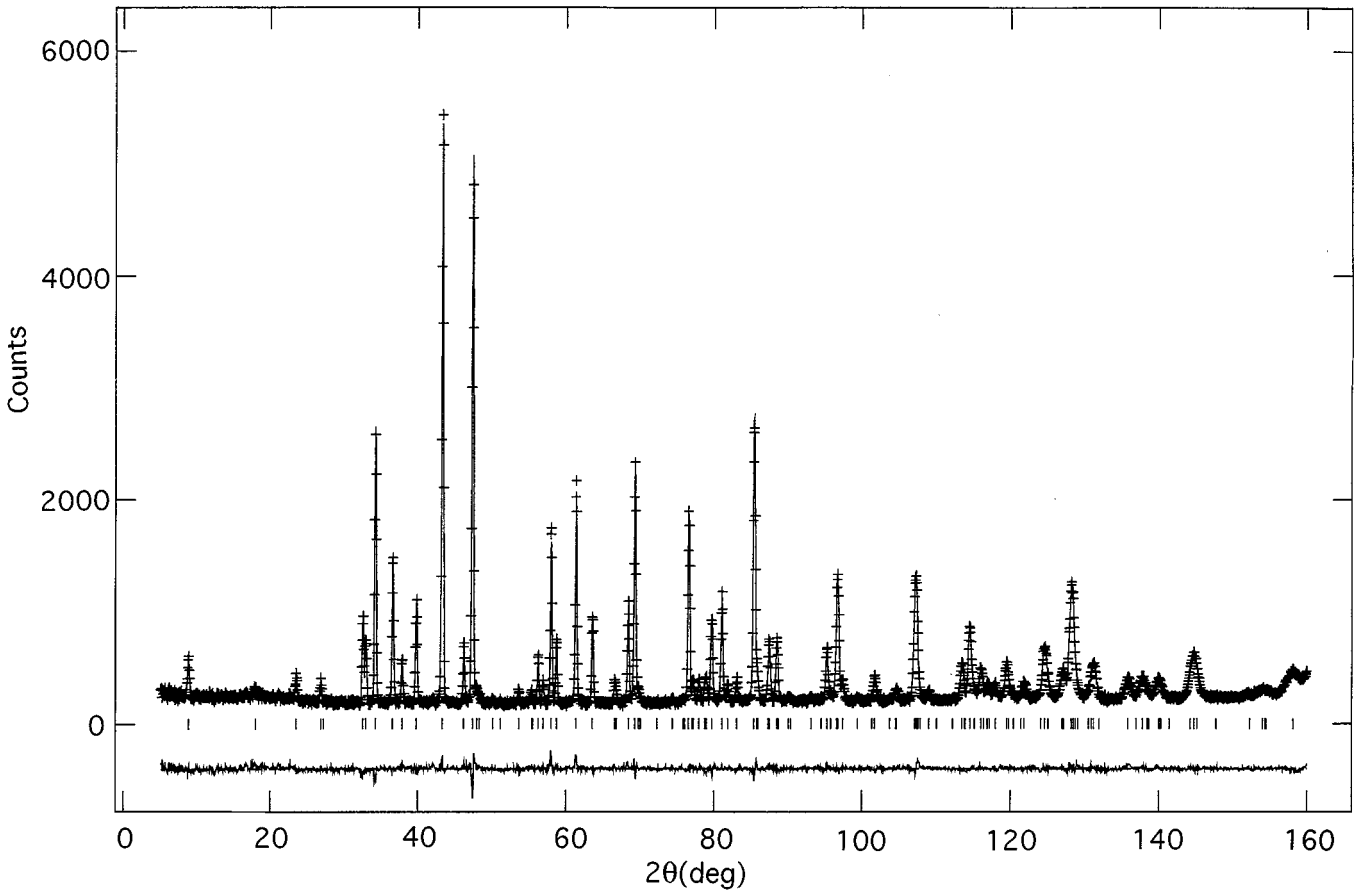

FIG. 5. The powder ND pattern at 295 K for $Sr_2Y_{0.8}Ca_{0.2}Co_2O_{6.00}$. All observed peaks are clearly reproduced by the calculation (solid curve) for the structural model. The calculated peak positions and the differential between the curves are presented as small vertical bars and a solid curve at the bottom, respectively.

in high-pressure oxygen. The lattice constants of the annealed phases were found by XRD to be $a = 3.766(1)$ Å and $c = 19.95(1)$ Å for $Sr_2Y_{0.8}Ca_{0.2}Co_2O_{6.79}$ and $a = 3.783(1)$ Å and $c = 19.81(1)$ Å for $Sr_2Y_{0.5}Ca_{0.5}Co_2O_{6.62}$. Shrinkage in both a-axis lattice constants (1.70% for $Sr_2Y_{0.8}Ca_{0.2}Co_2O_{6.79}$, and 1.33% for $Sr_2Y_{0.5}Ca_{0.5}Co_2O_{6.62}$) and an elongation in both c-axis lattice constants (1.68% for $Sr_2Y_{0.8}Ca_{0.2}Co_2O_{6.79}$, and 0.355% for $Sr_2Y_{0.5}Ca_{0.5}Co_2O_{6.62}$) were clearly observed. Although both oxygen accommodation and valence state changes are reflected in the c-axis change, the decrease in a-axis reflects a decrease in the Co–O bond length due to an increase in the formal oxidation state of Co.

MAGNETIC AND ELECTRICAL PROPERTIES

The temperature dependence of the magnetic susceptibility of $Sr_2Y_{0.8}Ca_{0.2}Co_2O_{5.92}$ at an applied magnetic field of 10 kOe is presented in Fig. 8. At approximately 300 K, a magnetic cusp was found, indicating an antiferromagnetically ordered state below the cusp temperature. Thermomagnetic hysteresis was not observed. A linear relation between magnetic field and magnetization was clearly observed in the vicinity of the magnetic cusp temperature, at 200 and 350 K, as expected for an AF spin structure (Fig. 8, insert). Therefore, the observed magnetically ordered stte can be considered to be a long range AF ordered state. This state is likely dominated by an AF superexchange interaction through the nearly 154 degree $Co^{2.52+}$–O–$Co^{2.52+}$ bond. The temperature dependence of the magnetic susceptibility of $Sr_2Y_{0.5}Ca_{0.5}Co_2O_{5.76}$ is also presented in Fig. 9. Due to the almost identical formal valences of Co (+2.52 for $Sr_2Y_{0.8}Ca_{0.2}Co_2O_{5.92}$ and +2.51 for $Sr_2Y_{0.5}Ca_{0.5}Co_2O_{5.76}$), the magnetic properties are almost identical with that of $Sr_2Y_{0.8}Ca_{0.2}Co_2O_{5.92}$.

All single-phase materials as made were found to be highly electrically insulating. The resistivity was found to decrease significantly for samples with oxygen content higher than obtained in the normal synthetic procedure. The materials, however, remained semiconducting. Heating the materials under very highly oxidizing conditions resulted in decomposition of the phase. However, it was found that

TABLE 2
Structural Parameters of $Sr_2Y_{0.8}Ca_{0.2}Co_2O_{6.00}$ at 295 K

Atoms	Structural parameters	
	a (Å)	3.82765(6)
	c (Å)	19.5795(3)
	V (Å^3)	286.86(1)
Y/Ca[a]	B (Å^2)	0.60(2)
Sr	z	0.32016(5)
	B (Å^2)	0.87(2)
Co	z	0.0965(1)
	B (Å^2)	0.74(4)
O(1)[b]	z	0.19507(6)
	B (Å^2)	1.02(2)
O(2)[c]	z	0.07433(4)
	B (Å^2)	1.04(2)

Note. Atomic positions ($I4/mmm$) are Y/Ca, 2b(0, 0, 1/2); Sr, 4e(0, 0, z); Co, 4e(0, 0, z); O(1), 4i(0, 0, z), and O(2), 8g(0, 1/2, z). The unit cell volume (V) was calculated from the lattice constants (a, b, and c). The final R factors were 4.07% (R_p) and 4.71% (R_{wp}).

[a]Occupancy of 80% Y and 20% Ca.

[b]The apical oxygen of the CoO_5 pyramid.

[c]The oxygen in the CoO_2 layer.

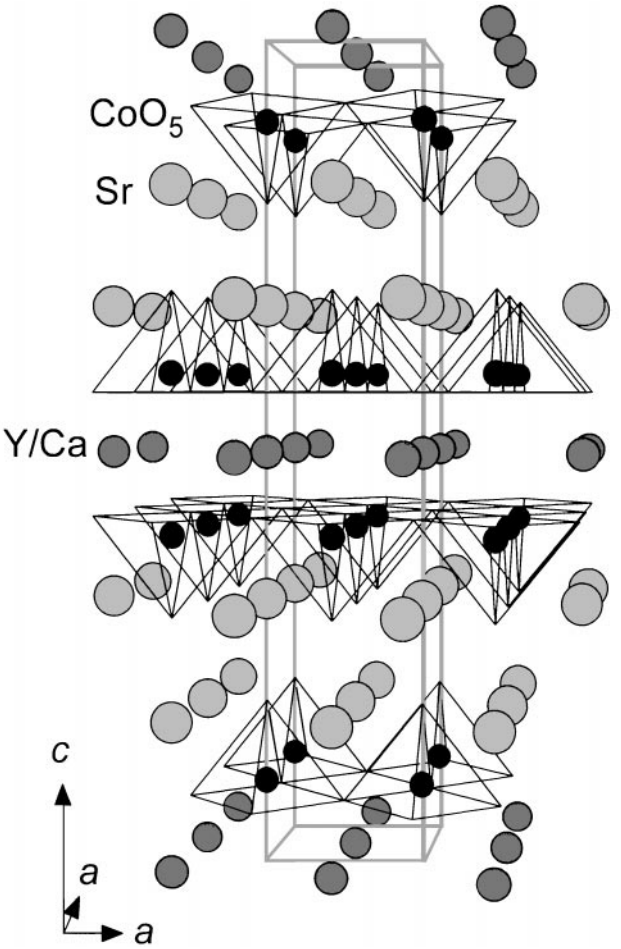

FIG. 6. Schematic structural view of $Sr_2Y_{0.8}Ca_{0.2}Co_2O_{6.00}$. Each polyhedron represents a CoO_5 pyramid. The Sr and the Y/Ca are shown as larger and smaller circles, respectively. The tetragonal unit cell is indicated by thick solid lines.

a final synthetic treatment of 430°C in high-pressure oxygen at 31.4 MPa resulted in an oxygen content, measured in the TGA, of 6.79 oxygens per f.u. for $Sr_2Y_{0.8}Ca_{0.2}Co_2O_y$ and 6.62 for $Sr_2Y_{0.5}Ca_{0.5}Co_2O_y$. These materials, though still semiconducting, had a room temperature resistivity of approximately 10^{-1} ohm-cm. The temperature dependence of the resistivity is shown in Figs. 10a and 10b. A plot of $\log \rho$ vs $1/T$ (Fig. 10a) shows nonlinear behavior for both materials. On the other hand, a variation of $\log \rho$ vs $1/T^{1/3}$ (Fig. 10b) shows almost linear behavior for $Sr_2Y_{0.8}Ca_{0.2}Co_2O_{6.79}$. This behavior is expected from variable range hopping conduction in a 2D system. The plots therefore suggest that thermally activated conduction across a gap is insufficient for understanding the electrical properties of $Sr_2(Y, Ca)Co_2^{3.4+}O_{6+\delta}$. Further study of the transport properties would be of interest.

In contrast to the AF properties of the $Co^{2.5+}$ phases, the high-pressure oxygen treated $Co^{3.4+}$ phases show singular magnetic properties. In Fig. 11, the applied magnetic field dependence of the thermomagnetic properties of $Sr_2Y_{0.8}Ca_{0.2}Co_2O_{6.79}$ is shown. The magnetic cusp temperature shifts toward lower temperatures and the thermomagnetic hysteresis decreases with increasing applied magnetic field. Similar behavior is also observed for $Sr_2Y_{0.5}Ca_{0.5}Co_2O_{6.62}$ (Fig. 12), where another magnetic anomaly at approximately 80 K was observed at the applied magnetic field of 0.1 kOe. We tentatively attribute the anomaly to a magnetic impurity in the sample, too low in concentration to be detected in the XRD study. In Fig. 13, the inverse magnetic susceptibility vs temperature is shown for both phases. Fitting with the Curie–Weiss law for the linear part between 300 and 400 K (solid line) gives an effective magnetic moment of 1.89 μ_B and a negative Weiss temperature of -314 K, indicating strongly AF interactions for

TABLE 3
Selected Interatomic Distances and Bond Angles for $Sr_2Y_{0.8}Ca_{0.2}Co_2O_{6.00}$ at 295 K

Atoms	Interatomic distance (Å)	Number of neighbors
Y/Ca–O(2)	2.4043(4)	8
Sr–O(1)	2.448(2)	1
	2.7228(2)	4
Sr–O(2)	2.8172(8)	4
Co–O(1)	1.928(3)	1
Co–O(2)	1.9628(6)	4
Atoms		Bond angle (degree)
O(1)–Co–O(2)		102.83(8)
O(2)–Co–O(2)		87.17(8)
Co–O(2)–Co		154.4(2)

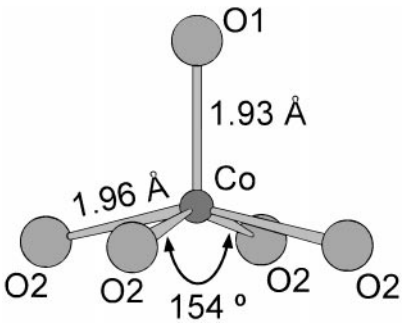

FIG. 7. Schematic view of a CoO_5 pyramid at 295 K of $Sr_2Y_{0.8}Ca_{0.2}Co_2O_{6.00}$.

$Sr_2Y_{0.8}Ca_{0.2}Co_2O_{6.79}$. The Curie–Weiss law could not be applied for $Sr_2Y_{0.5}Ca_{0.5}Co_2O_{6.62}$ due to the limitation of the experimentally available temperature range. The magnetic field dependence of magnetization at 50 K (Fig. 14a), a temperature slightly higher than the magnetic cusp temperature, suggests the presence of ferromagnetic (FM) correlations in both phases. At 5 K, below the magnetic cusp temperature, magnetic hysteresis, also characteristic of the presence of FM spin correlations, was clearly observed for both phases (Fig. 14b). At the same temperature, 5 K, a time dependent relaxation of the magnetization (Fig. 15) was observed. This relaxation was found to obey the Kohlrausch-law, which is the behavior expected for a glassy system with a distribution of relaxation times (12). The values of the fitting parameters obtained $a = 2.115$ and $n = 3.281 \times 10^{-2}$ for $Sr_2Y_{0.8}Ca_{0.2}Co_2O_{6.79}$, and $a = 2.248$

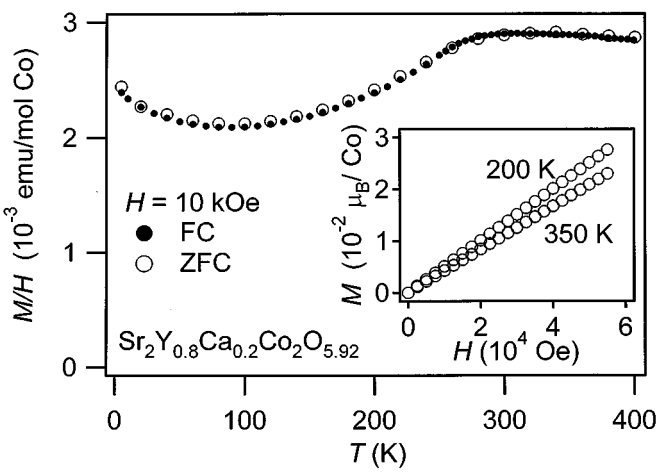

FIG. 8. Temperature dependence of the magnetic susceptibility of $Sr_2Y_{0.8}Ca_{0.2}Co_2O_{5.92}$. After cooling the polycrystalline sample to 5 K, a magnetic field of 10 kOe was applied. The sample was then slowly warmed up to 400 K (zero field cooling, ZFC) and again slowly cooled down to 5 K (field cooling, FC). The magnetic field dependence of magnetization was measured at 200 K and 350 K up to 55 kOe (insert).

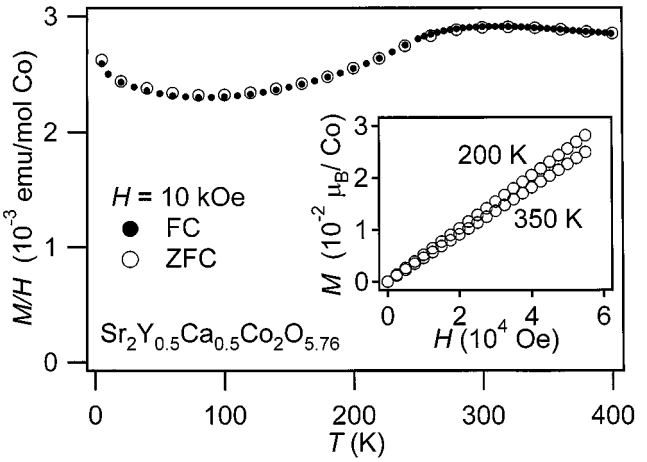

FIG. 9. Temperature dependence of the magnetic susceptibility of $Sr_2Y_{0.5}Ca_{0.5}Co_2O_{5.76}$. After cooling the polycrystalline sample to 5 K, a magnetic field of 10 kOe was applied. The sample was then slowly warmed up to 400 K (zero field cooling, ZFC) and again slowly cooled down to 5 K (field cooling, FC). The magnetic field dependence of magnetization was measured at 200 K and 350 K up to 55 kOe (insert).

and $n = 2.686 \times 10^{-2}$ for $Sr_2Y_{0.5}Ca_{0.5}Co_2O_{6.62}$ in the formula $M/M_0 = \exp(-at^n)$, where M is magnetization, M_0 is the magnetization at $t = 0$, and t is time, are consistent with what is expected for systems like this one (12).

DISCUSSION AND CONCLUSION

The observed effective magnetic moment of 1.89 μ_B for $Co^{3.39+}$ in $Sr_2Y_{0.8}Ca_{0.2}Co_2O_{6.79}$ is expected to the average of those of the Co^{3+} and Co^{4+} present in the ratio 0.61:0.39 in this compound. Several possible combinations of spin states are possible: three kinds of $3d^6$ states ($t_{2g}^6\, e_g^0$, $S = 0$; $t_{2g}^5\, e_g^1$, $S = 1$; $t_{2g}^4\, e_g^2$, $S = 2$) for Co^{3+}, and three kinds of $3d^5$ states ($t_{2g}^5\, e_g^0$, $S = 1/2$; $t_{2g}^4\, e_g^1$, $S = 3/2$; $t_{2g}^3\, e_g^2$, $S = 5/2$) for Co^{4+}. None of the combinations yield an average moment close to the observed value based on the formula $2 \times (S(Co^{3+}) \times (S(Co^{3+}) + 1))^{-1/2} \times 0.61 + 2 \times (S(Co^{4+}) \times (S(Co^{4+}) + 1))^{-1/2} \times 0.39)$, employed for the case when distinct Co^{3+} and Co^{4+} ions are statically distributed over the available sites. The closest value obtained from the calculation, 1.51 μ_B, where $S(Co^{3+}) = 0$ ($t_{2g}^6\, e_g^0$) and $S(Co^{4+}) = 3/2$ ($t_{2g}^4\, e_g^1$), is unreasonably small compared to the observed value. The second closest value, where $S(Co^{3+}) = 0$ ($t_{2g}^6\, e_g^0$) and $S(Co^{4+}) = 5/2$ ($t_{2g}^3\, e_g^2$), and the third closest value, where $S(Co^{3+}) = 1$ ($t_{2g}^5\, e_g^1$) and $S(Co^{4+}) = 1/2$ ($t_{2g}^5\, e_g^0$), are fairly large, 2.31 μ_B and 2.40 μ_B, respectively. On the other hand, calculation based on an alternative assumption, using the formula, $2 \times (S'(S' + 1))^{-1/2}$, where $S' = S(Co^{3+}) \times 0.61 + S(Co^{4+}) \times 0.39$, $S(Co^{3+}) = 0$ ($t_{2g}^6\, e_g^0$), and $S(Co^{4+}) = 3/2$ ($t_{2g}^4\, e_g^1$), gives a very close value, 1.93 μ_B, to the observed value. The formula comes from the assumption

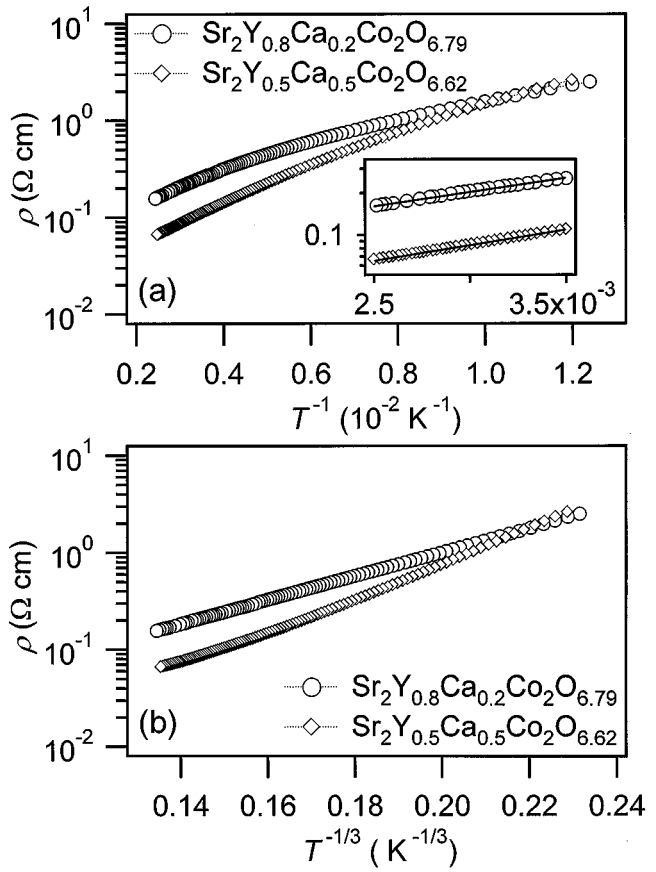

FIG. 10. Temperature dependence of the resistivity of $Sr_2Y_{0.8}Ca_{0.2}Co_2O_{6.79}$ and $Sr_2Y_{0.5}Ca_{0.5}Co_2O_{6.62}$. Plots of $\log \rho$ vs $1/T$ (a) and $\log \rho$ vs $1/T^{1/3}$ (b) are shown. The energy gaps estimated from the linear part in $\log \rho$ vs $1/T$ plot (insert, (a)) are 41.0 meV for $Sr_2Y_{0.8}Ca_{0.2}Co_2O_{6.79}$ and 43.6 meV for $Sr_2Y_{0.5}Ca_{0.5}Co_2O_{6.62}$.

of an average magnetic moment on each Co-site. The combination is the low spin state for Co^{3+} and the intermediate spin state for Co^{4+}. The next closest value based on the

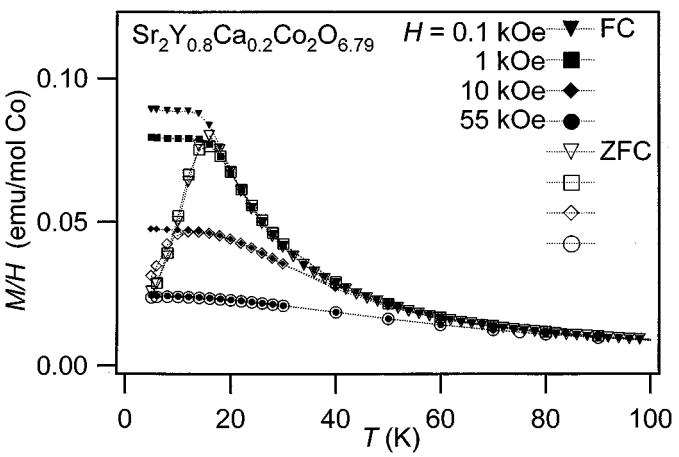

FIG. 11. Temperature and magnetic field dependence of the magnetic susceptibility of $Sr_2Y_{0.8}Ca_{0.2}Co_2O_{6.79}$.

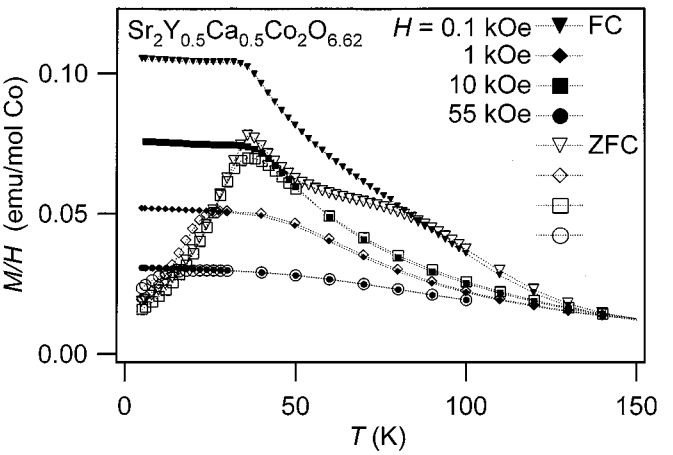

FIG. 12. Temperature and magnetic field dependence of the magnetic susceptibility of $Sr_2Y_{0.5}Ca_{0.5}Co_2O_{6.62}$.

second assumption, 2.41 μ_B, results from the combination of the intermediate spin state and the low spin state: Co^{3+} (t_{2g}^5 e_g^1, $S = 1$) and Co^{4+} (t_{2g}^5 e_g^0, $S = 1/2$). The third closest value, 2.78 μ_B, for the combination of Co^{3+} (t_{2g}^6 e_g^0, $S = 0$) and Co^{4+} (t_{2g}^3 e_g^2, $S = 5/2$) is far from the observed value. Because it is unclear which of the spin distribution assumptions is appropriate to describe the mixed valence Co, and the fact that the intermediate spin state, which we suggest for the Co^{4+} (e.g., t_{2g}^4 e_g^1, $S = 3/2$), is quite unusual (low spin or high spin state are more commonly observed), further study would be required to clarify the spin state of the mixed valence Co in the present materials. Only for $LaCo^{3+}O_3$ has the possibility of an intermediate spin state been suggested (13, 14).

A magnetically glassy transition was observed at lower temperature for both oxidized $Co^{3.4+}$ phases. The static

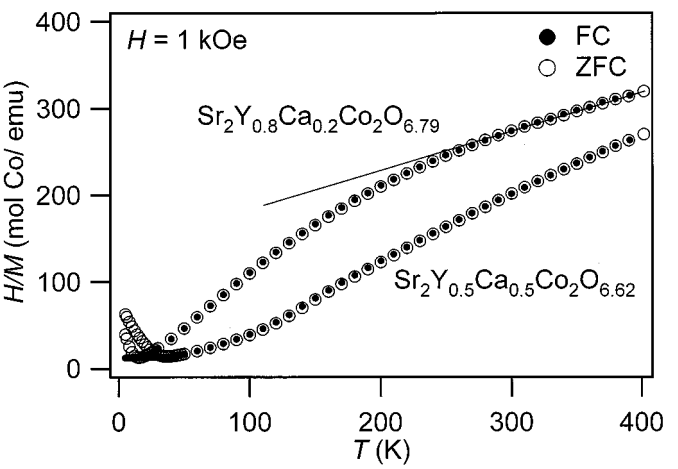

FIG. 13. Inverse magnetic susceptibility vs temperature of $Sr_2Y_{0.8}Ca_{0.2}Co_2O_{6.79}$ and $Sr_2Y_{0.5}Ca_{0.5}Co_2O_{6.62}$. The Curie–Weiss law fit for the linear part is indicated by the solid line: the effective magnetic moment is 1.89 μ_B and the Weiss temperature is -314 K.

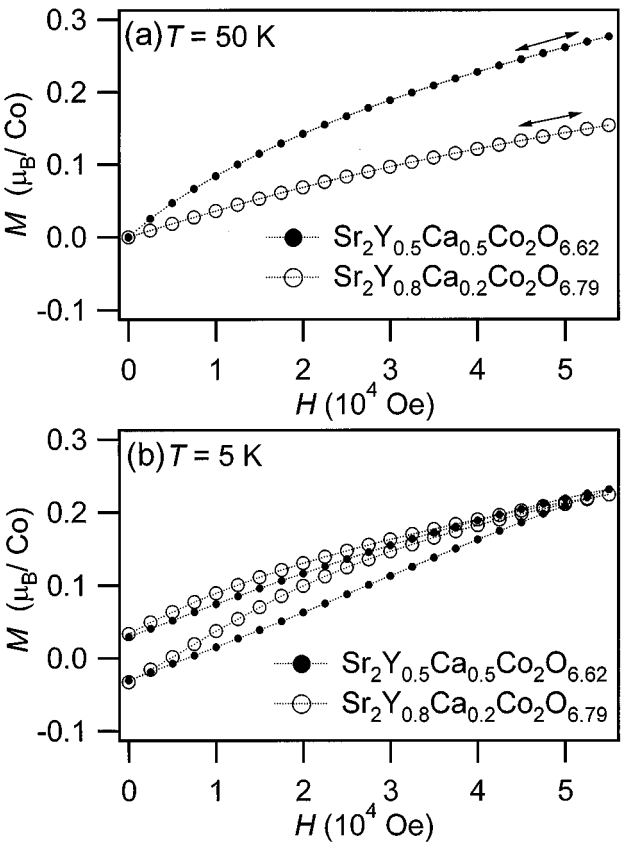

FIG. 14. Magnetic field dependence of the magnetization of $Sr_2Y_{0.8}Ca_{0.2}Co_2O_{6.79}$ and $Sr_2Y_{0.5}Ca_{0.5}Co_2O_{6.62}$ at 50 K (a) and 5 K (b). Saturation in magnetization was not observed to the highest magnetic field (55 kOe); however, ferromagnetic interaction is detected clearly for both phases.

magnetic susceptibility data are on the whole consistent with the properties of a spin glass. As shown in Figs. 13, 14a, and 14b, two kinds of signs of spin interaction were found: the negative Weiss temperature suggests an AF interaction and the magnetic field dependence of magnetization suggests an FM interaction. These two kinds of interactions may be competing with each other, frustrating the long-range arrangement of spins. Also, the presence of the excess oxygen in a disordered manner in the planes between the CoO_5 pyramids may result in a random distribution of Co^{3+} and Co^{4+}, frustrating the magnetic order. On the other hand, the parent materials $Sr_2Y_{0.8}Ca_{0.2}Co_2O_{5.92}$ and $Sr_2Y_{0.5}Ca_{0.5}Co_2O_{5.76}$ display a long-range ordered AF state. For these materials there is no FM interaction. The FM interaction, then, is introduced by the oxidization of the phases. The oxygens introduced are likely accommodated in the Y/Ca layer, helping to establish FM bonds in addition to the AF bonds (15, 16). We expect that the cobalt bonded to this extra oxygen will move toward the oxidized Y/Ca layer, resulting in more regular bond angles. It is also possible that the sign of the superexchange interaction between nearest neighbor magnetic moments for some Co sites changes to positive due to the increment of the formal valence of Co from 2.5+ to 3.4+, i.e., the $d^6 - d^7$ system changes to a $d^5 - d^6$ system (15, 16). Study of the local crystal structure and nonlinear magnetic susceptibility to further characterize the magnetically glassy state in these materials would be of interest.

All materials made in this study were found to be electrically insulating. At the compositions $Sr_2Y_{0.8}Ca_{0.2}Co_2^{2.51+}O_{5.92}$ and $Sr_2Y_{0.5}Ca_{0.5}Co_2^{2.52+}O_{5.76}$, metallic behavior may be expected due to partial band filling for the mixed electronic valence between Co^{2+} and Co^{3+}. Insulating behavior was found, however, possibly due to 2D-localization of the electrons. A band structure calculation to help clarify the origin of the insulating properties would be of interest. For $Sr_2Y_{0.8}Ca_{0.2}Co_2^{3.39+}O_{6.79}$ and $Sr_2Y_{0.5}Ca_{0.5}Co_2^{3.37+}O_{6.62}$, the resistivities decrease to approximately 10^{-1} ohm-cm at room temperature and show nonlinear behavior in $\log\rho$ vs $1/T$ plots. The carrier concentration of the phases was significantly changed due to the oxidization: approximately 0.9 holes per Co were formally doped into the compounds. More precise control in carrier concentration would be required to investigate the insulating properties and to obtain much more highly carrier doped phases, where metallic properties may be possible.

A spin glass transition is evidence of the existence of spin frustration even though spins are frozen below the transition temperature. Evidence of the coexistence of FM and AF interactions, which may induce the frustration, was found for $Sr_2Y_{0.8}Ca_{0.2}Co_2O_{6.79}$ and $Sr_2Y_{0.5}Ca_{0.5}Co_2O_{6.62}$. To explore the character of the metallic state in the frustrated spin system, which would be of interest, further chemical modification is essential. Further studies are in progress.

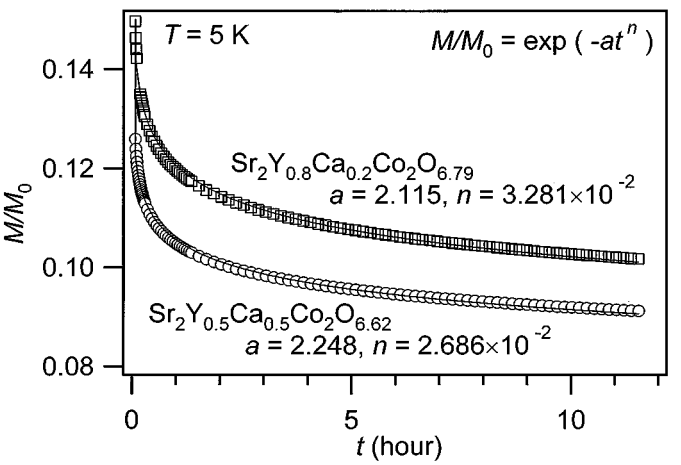

FIG. 15. Magnetic relaxation phenomena of $Sr_2Y_{0.8}Ca_{0.2}Co_2O_{6.79}$ (open squares) and $Sr_2Y_{0.5}Ca_{0.5}Co_2O_{6.62}$ at (open circles) at 5 K. After cutting off the magnetic field of 55 kOe ($t = 0$), the time dependence of the magnetization was measured. Data for each phase were normalized by the magnetization at $t = 0$. Solid lines show fits of the data to the Kohlrausch law.

ACKNOWLEDGMENTS

This work was supported in part by Grant NSF DMR97-25979 and one of us (K.Y.) was supported by an Overseas Research Fellowship, administered by the Japan Science and Technology Corporation.

REFERENCES

1. Landolt-Bàrnstein, new series III/21a: "Superconductors: Transition Temperatures and Characterization of Elements, Alloys and Compounds," 1990.
2. Y. Maeno, H. Hashimoto, K. Yoshida, S. Nishizaki, T. Fujita, J. G. Bednorz, and F. Lichtenberg, *Nature* **372,** 532 (1994).
3. R. J. Cava, H. W. Zandbergen, B. Batlogg, H. Eisaki, H. Takagi, J. J. Krajewski, W. F. Peck, Jr., and E. M. Gyorgy, *Nature* **372,** 759 (1994).
4. R. J. Cava, H. Takagi, B. Batlogg, H. W. Zandbergen, J. J. Krajewski, W. F. Peck, Jr., R. B. van Dover, R. J. Felder, T. Siegrist, S. A. Carter, K. Mizuhashi, J. O. Lee, H. Eisaki, and S, Uchida, *Nature* **367,** 146 (1994).
5. R. J. Cava, H. Takagi, H. W. Zandbergen, J. J. Krajewski, W. F. Peck, Jr., T. Siegrist, B. Batlogg, R. B. van Dover, R. J. Felder, K. Mizuhashi, J. O. Lee, H. Eisaki, and S, Uchida, *Nature* **367,** 252 (1994).
6. G. M. Luke, Y. Fudamoto, K. M. Kojima, M. I. Larkin, J. Merrin, B. Nachumi, Y. J. Uemura, Y. Maeno, Z. Q. Mao, Y. Mori, H. Nakamura, and M. Sigrist, *Nature* **394,** 558 (1998).
7. H. Takagi, M. Nohara, and R. J. Cava, *Physica B* **237,** 292 (1997).
8. R. J. Cava, B. Batlogg, R. B. van Dover, J. J. Krajewski, J. V. Waszczak, R. M. Fleming, W. F. Peck, Jr., L. W. Rupp, Jr., P. Marsh, A. C. W. P. James, and L. F. Schneemeyer, *Nature* **345,** 602 (1990).
9. A. C. Larson and R. B. Von Dreele, Los Alamos National Laboratory Report LAUR086-748 (1990).
10. R. D. Shannon, *Acta Crystallogr. Sec. A* **32,** 751 (1976).
11. R. J. Cava, R. B. van Dover, B. Batlogg, J. J. Krajewski, L. F. Schneemeyer, T. Siegrist, B, Hessen, S. H. Chen, W. F. Peck, and L. W. Rupp, *Physica C* **185,** 180 (1991).
12. K. L. Ngai, *J. Chem. Phys.* **109,** 6982 (1998).
13. M. A. Korotin, S. Yu. Ezhov, I. V. Solovyev, V. I. Anisimov, D. I. Khomskii, and G. A. Sawatzky, *Phys. Rev. B* **54,** 5309 (1996).
14. T. Saitoh, T. Mizokawa, A. Fujimori, M. Abbate, Y. Takeda, and M. Takano, *Phys. Rev. B* **55,** 4257 (1997).
15. J. B. Goodenough, *Phys. Rev.* **100,** 564 (1955).
16. J. Kanamori, *J. Phys. Chem. Solids* **10,** 87 (1959).